Vol. 634: 45–61, 2020
https://doi.org/10.3354/meps13182

MARINE ECOLOGY PROGRESS SERIES
Mar Ecol Prog Ser

Published January 23

Acetate-utilizing microbial communities revealed by stable-isotope probing in sediment underlying the upwelling system of the Ulleung Basin, East Sea

Hyeyoun Cho[1], Bomina Kim[1], Jin-Sook Mok[1], Ayeon Choi[1], Bo Thamdrup[2], Jung-Ho Hyun[1,*]

[1]Department of Marine Sciences and Convergent Technology, Hanyang University, 55 Hanyangdaehak-ro, Ansan, Gyeonggi-do 15588, South Korea

[2]Nordic Center for Earth Evolution, Institute of Biology, University of Southern Denmark, Campusvej 55, 5230 Odense M, Denmark

ABSTRACT: Molecular analyses and biogeochemical measurements were combined to investigate the microbial communities associated with major terminal electron accepting processes and acetate oxidation at 2 contrasting sediments on the continental shelf (EB1) and basin (EB6) of the Ulleung Basin, East Sea. At EB1, sulfate reduction (SR) and iron reduction (FeR) dominated organic carbon (C_{org}) oxidation, accounting for 65 and 25% of anaerobic C_{org} oxidation, respectively. In contrast, manganese reduction (MnR) was responsible for >50% of anaerobic C_{org} mineralization at manganese oxide-rich EB6. Members of *Desulfobacteraceae*, known as putative sulfate-reducing bacteria (SRB), constituted a major C_{org}-oxidizing clade (22% of *Bacteria*) at EB1. Meanwhile, putatively Mn-reducing bacteria affiliated with *Colwelliaceae*, *Shewanellaceae* and *Oceanospirillaceae* were abundant in EB6 (8% of *Bacteria*). RNA-stable isotope probing (RNA-SIP) further identified *Arcobacter* as acetate-oxidizers associated with FeR, while no SRB were labeled at EB1. At EB6, microorganisms affiliated with *Colwelliaceae* and *Oceanospirillaceae* were identified as putative Mn-reducing acetate-oxidizers. Interestingly, at both sites, *Thaumarchaeota* were labeled with ^{13}C derived from acetate during the anoxic incubations. The results from RNA-SIP give new insights into the biogeochemical and ecological role of *Arcobacter* in FeR, and the metabolic activity of *Thaumarchaeota* under anoxia. As the upwelling intensity in the UB declines due to the rapid warming of surface waters, our results are relevant for evaluation of future changes in benthic biogeochemical processes and microbial communities in response to the variations of water-column productivity.

KEY WORDS: Acetate-oxidizing bacteria · Benthic microbial communities · East Sea · Organic carbon oxidation · RNA-SIP · Ulleung Basin

1. INTRODUCTION

In most marine shelf sediments, oxygen is depleted within the top few mm depth, and thus organic matter remineralization is to a large extent performed by various anaerobic microorganisms utilizing different electron acceptors such as nitrate, manganese oxide, iron oxide and sulfate (Thamdrup & Canfield 2000, Canfield et al. 2005, Orcutt et al. 2011). In general, due to the high concentration of sulfate (ca. 28 mM) in marine environments, sulfate reduction (SR) is typically responsible for most of the anaerobic organic carbon (C_{org}) oxidation (Jørgensen & Kasten 2006). However, in certain environments where man-

*Corresponding author: hyunjh@hanyang.ac.kr

ganese- and iron oxides are abundant and rapidly recycled, Mn(IV)- and Fe(III)-reduction play more significant roles in C_{org} oxidation relative to SR (Canfield et al. 1993, Jensen et al. 2003, Vandieken et al. 2006, Hyun et al. 2009b, 2017). Conversely, while denitrification is important for the removal of fixed nitrogen in various marine environments (Henriksen et al. 1993, Granger et al. 2011), it typically contributes little to C_{org} oxidation (Hyun et al. 2017, Na et al. 2018). Since the end-products or intermediates of these terminal electron-accepting processes (TEAPs), i.e. Mn^{2+}, Fe^{2+}, H_2S and NH_4^+, can be rapidly recycled within the system by re-oxidation, precipitation and biological uptake (Canfield et al. 2005), geochemical analysis alone may not provide complete information on the major C_{org} oxidation pathways prevailing in certain conditions (Jørgensen 2006). Since microorganisms are potent biogeochemical agents participating in most elemental cycles (Ehrlich 1990, Canfield et al. 2005), elucidating major prokaryotic populations that are directly responsible for specific metabolic processes is essential to better understand the major biogeochemical processes that determine the behavior and distribution of elements in marine sediments (Bowman & McCuaig 2003, Inagaki et al. 2006, Jorgensen et al. 2012)

Although rapid development in molecular techniques has provided new information on microbial community composition and their function in nature without cultivation (Amann et al. 1995, Rotthauwe et al. 1997), it has been difficult to elucidate which microbial groups are responsible for specific biogeochemical transformations. Stable isotope probing (SIP) methods in combination with biogeochemical analyses have been used as relevant tools for the identification of microorganisms that are actively incorporating specific substrates of interest into microbial biomass in natural environments, thereby enabling a direct link between substrate utilization and specific prokaryotes (Radajewski et al. 2000, Webster et al. 2010, Vandieken et al. 2012, Berg et al. 2013, Vandieken & Thamdrup 2013). Acetate, a key end-product of the anaerobic food chain, is a major electron donor for anaerobic microbial carbon oxidation processes (Canfield et al. 2005), and thus has been used in many biogeochemical and microbiological studies for understanding carbon oxidation processes related to the reduction of nitrate, Mn, Fe and sulfate (Lovley & Phillips 1988, Parkes et al. 1989, Finke et al. 2007, Hyun et al. 2009b, Lentini et al. 2012). Especially, since any organic carbon is no longer produced by acetate oxidation, it is particularly useful for RNA-SIP studies to elucidate the microbial consortia associated with specific TEAPs in marine environments (Vandieken et al. 2012, 2013, Berg et al. 2013, Vandieken & Thamdrup 2013).

The Ulleung Basin (UB), located in the southwest of the East Sea, is characterized by high biological productivity resulting from coastal upwelling along the southeast Korean peninsula (Hyun et al. 2009a, Yoo & Park 2009). As a result of the high export flux (Kim et al. 2009), surface sediment of the UB exhibits high C_{org} content (>2.5% dry wt.; Lee et al. 2008) and microbial metabolic activities are comparable to those reported from similar depths of the highly productive Peruvian and Chilean upwelling regions (Hyun et al. 2010, 2017). Thus, the UB is regarded as a biogeochemical hotspot where significant turnover of organic matter and nutrient regeneration takes place (Hyun et al. 2017). Previous biogeochemical studies reported that SR was the major C_{org} oxidation pathway along the continental margins of the UB, whereas manganese reduction (MnR) was a dominant TEAP in the center where surface sediments were enriched with manganese oxides (>200 µmol cm^{-3}) (Hyun et al. 2010, 2017). Subsequent microbiological studies using RNA-SIP indicated bacteria affiliated with gammaproteobacterial *Oceanospirillaceae* and *Colwellia*, as well as epsilonproteobacterial *Arcobacter* were involved in MnR in the manganese oxide-rich basin center (Vandieken et al. 2012). However, the spatial variability of microbial communities and acetate-oxidizing bacterial and archaeal communities remains to be elucidated in continental shelf and deep basin sediments of the UB, where rapid C_{org} turnover and nutrient regeneration occurs by different TEAPs including the reduction of Mn, Fe and sulfate (Hyun et al. 2010, 2017).

Based on a combination of comprehensive biogeochemical analyses on C_{org} oxidation pathways and molecular ecological analyses, the objectives of this study were to (1) characterize the metabolically active anaerobic prokaryotic communities with special focus on the microbes responsible for major TEAPs, and (2) elucidate the acetate-utilizing microbial communities using RNA-SIP in the sediments underlying highly productive upwelling system of the UB.

2. MATERIALS AND METHODS

2.1. Study area, sediment sampling and handling

The East Sea (often referred to as the Japan Sea) is a marginal sea surrounded by Korea, Japan and Russia in the far eastern part of the Eurasian continent

(Fig. 1), and consists of 3 deep basins: Japan Basin (JB), Yamato Basin (YB) and UB. Sediment samples were collected using a box corer at 2 contrasting sites: one on the continental shelf (EB1) and the other in center (EB6) of the UB (see Table 1, Fig. 1). Subsamples for geochemical analyses, total anaerobic C_{org} oxidation rate measurements and slurry incubations for RNA-SIP were collected using acryl core liners (6–9 cm inner diameter [i.d.]). Sediment cores for measuring sulfate reduction rates (SRRs) were collected in triplicate using acryl core liners (3 cm i.d.). Sub-cores for pore-water analyses were sectioned in a glove bag filled with N_2 gas. To analyze pore-water constituents, sectioned sediment samples were centrifuged at 2600 × *g* for 10 min, and collected pore-water was filtered through 0.2 µm cellulose acetate syringe filters (Advantec, Toyo Roshi Kaisha) in a glove bag. Pore-waters for measuring Fe^{2+} and Mn^{2+} were fixed with 12 M HCl. The sediment remaining after the collection of pore-water was frozen at –25°C for future analysis of the solid-phase.

2.2. Rate of anaerobic C_{org} oxidation and iron and sulfate reduction

The anaerobic C_{org} mineralization rate was determined experimentally based on the procedures of Canfield et al. (1993) and Thamdrup & Canfield (1996). Briefly, sediment cores were transferred to a glove bag filled with N_2 gas and sliced in 2 cm intervals to a depth of 6 cm. Sediment from parallel sections was pooled, mixed and loaded into 50 ml conical tubes. The tubes were incubated in the dark at *in situ* temperature in larger N_2-filled bags to ensure anoxic conditions. Two tubes were then withdrawn at regular intervals and pore-water was extracted as described above. For dissolved inorganic carbon (DIC) analysis, we collected 2 ml aliquots into glass vials without head space, fixed with 18 µl of $HgCl_2$ (125 mM), and stored at 4°C until analysis within 4 wk. The total anaerobic C_{org} oxidation rate was determined by linear regression of the accumulation of DIC after correcting for $CaCO_3$ precipitation according to Thamdrup et al. (2000) (Fig. S1 in the Supplement at www.int-res.com/articles/suppl/m634p045_supp.pdf).

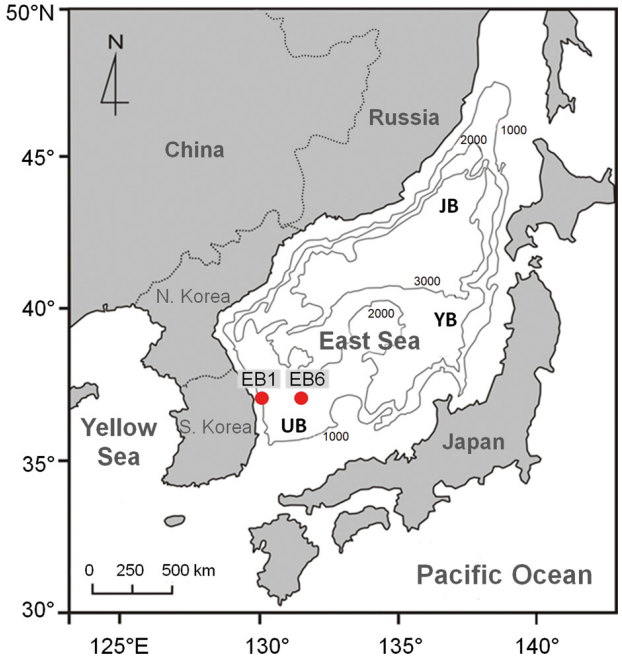

Fig. 1. Sampling sites in the continental shelf (EB1) and center (EB6) of the Ulleung Basin. Contour lines: water depth (in m)

Iron reduction rates (FeRR) were determined by linear regression of the increase in solid-phase oxalate-extractable Fe(II) concentration [$Fe(II)_{(oxal)}$] with time during the incubation of the sediment for measuring anaerobic C_{org} oxidation. After pore-water retrieval from the anaerobic C_{org} mineralization experiment, the remaining sediment was homogenized and subsampled under a N_2 atmosphere for Fe extraction. Solid-phase $Fe(II)_{(oxal)}$ was extracted in oxalate as described below. The dissimilatory microbial FeRRs were derived by subtracting the abiotic iron reduction (FeR) coupled to the oxidation of sulfide produced by SR (Kostka et al. 2002, Hyun et al. 2009b).

SRRs were determined on intact cores using the radiotracer method of Jørgensen (1978). The sediment samples were injected with 5 µl of radiolabeled sulfate ($^{35}S\text{-}SO_4^{2-}$, 15 kBq µl^{-1}; Amersham Biosciences) diluted in sterilized NaCl solution (3.0%), and incubated 8–24 h at *in situ* temperature. At the end of the incubation, the sediment was fixed in zinc acetate (20%) and frozen until processed in the laboratory. The reduced ^{35}S was recovered using distillation with a boiling acidic Cr^{2+} solution according to Fossing & Jørgensen (1989).

2.3. Slurry incubation for SIP

For the slurry incubations, sediment from 0–3 cm depth at each study site was pooled from parallel cores and mixed with filtered anoxic bottom water (1:1, sediment:bottom water) in a glove bag (Atmosbag, Sigma-Aldrich) filled with N_2 gas. The sediment slurries were distributed into three 500 ml amber glass bottles closed with thick butyl stoppers. Two of

the slurries were amended every day with approximately 170 µM (final concentration) of unlabeled (^{12}C) or (U-^{13}C)-labeled acetate, respectively. The third slurry was incubated as a control without acetate addition. The sediment slurries were incubated at near *in situ* temperature (1–3°C) in the dark for 17 d. During the incubations, subsamples for analyses of pore-water and solid phase constituents, and RNA extraction were collected just before each addition of acetate in the N_2 gas filled glove bag. For analyses of Fe^{2+}, Mn^{2+}, Ca^{2+} and DIC, aliquots of the sediment slurries were centrifuged in 15 ml centrifuge tube at 2600 × *g* for 10 min. Supernatant waters were filtered through 0.2 µm filters and stored as described above. To measure acetate concentration, supernatant was filled into glass vials without filtration, and stored frozen until analyzed. The sediment remaining after the collection of pore-water was frozen at −25°C for future analysis of solid Fe in the slurries.

2.4. Analyses of pore-water and solid-phase constituents

Total DIC and NH_4^+ in pore-water were measured by flow injection analysis (FIA; Hall & Aller 1992). The NO_x (NO_2^- + NO_3^-) concentration was measured using an auto-analyzer (Proxima, Alliance). Dissolved Fe^{2+} was determined by colorimetry with ferrozine (Stookey 1970). Dissolved Mn^{2+} and Ca^{2+} were analyzed by inductive coupled plasma-atomic emission spectrometry (ICP-AES; Optima 3300DV, Perkin-Elmer) and a flame atomic absorption spectrometer (SpectrAA 220/FS, Varian), respectively. Acetate concentration was measured according to the method in Ding et al. (2006). We used an Atlantis^{TM} C_{18} column (4.6 mm × 250 mm × 5 µm, Waters Company) and an Agilent 1200 series HPLC system (Agilent Technologies). The standard solutions were acquired from the stock solutions by dilution from an organic acids kit (Sigma-Aldrich).

The contents of total organic carbon (TOC) and total nitrogen (TN) in the sediment were measured using a CHN analyzer (EA 1110, CE Instruments) after removing $CaCO_3$ using 12 N HCl. Oxalate-extractable Fe(III) [$Fe(III)_{(oxal)}$], representing poorly crystalline Fe(III) oxides, was determined by a combination of 2 extractions (Thamdrup & Canfield 1996). Total oxalate-extractable Fe [Fe(II) + Fe(III)] in the sediments was extracted from air-dried sediment in a 0.2 M oxic oxalate solution (pH 3) for 4 h (Thamdrup & Canfield 1996), and $Fe(II)_{(oxal)}$ was extracted from fresh sediment in anoxic oxalate (Phillips & Lovley 1987). The concentrations of the oxalate-extractable total Fe (total $Fe_{(oxal)}$) and $Fe(II)_{(oxal)}$ were determined by colorimetry with ferrozine (Stookey 1970). $Fe(III)_{(oxal)}$ was defined as the difference between total $Fe_{(oxal)}$ and $Fe(II)_{(oxal)}$. Particulate Mn was extracted with dithionite-citrate-acetic acid (DCA; pH 4.8) for 4 h from air-dried sediment and was determined by ICP-AES. The DCA extraction for manganese ($Mn_{(DCA)}$), is expected to be more selective for manganese oxides (Canfield et al. 1993).

2.5. RNA extraction and density gradient centrifugation

RNA was extracted from approximately 2 g of frozen sediment (–80°C) from different sampling days (Day 0, 5, 7 and 13) of the 3 treatments with a PowerSoil Total RNA Isolation Kit in combination with a DNA Elution Accessory Kit (MOBIO). The RNA was further purified with a QIAGEN AllPrep DNA/RNA Mini Kit and quantified with RiboGreen RNA-quantification kit (Invitrogen). Portions of 600 ng total RNA were separated by density gradient ultracentrifugation and the gradients were fractionated and further processed as described by Whiteley et al. (2007). The RNA concentration in each fraction was determined using the RiboGreen RNA-quantification kit. Relative ratio of RNA concentration in each gradient is presented in Fig. S2.

2.6. Terminal restriction fragment length polymorphism

RNA of selected SIP fractions and total RNA from the Day 0-slurry were reverse transcribed into cDNA using primer 907R targeting bacterial 16S rRNA genes and primer 958R targeting archaeal 16S rRNA genes, with Sensiscript Reverse Transcription Kit (QIAGEN). A light fraction in each gradient was selected as the fraction with maximum RNA concentration around density 1.81 g ml^{-1}, whereas a heavy fraction was chosen as the fraction with highest RNA concentration along the gradient with a density greater than 1.82 g ml^{-1}. The cDNA was amplified using PCR with 8F (6-FAM-labeled) and 907R primers and 21F (6-FAM-labeled) and 958R primers. Amplicons were purified with a PCRquick-spin^{TM} PCR purification kit (iNtRON Biotechnology), and the concentrations were determined using NanoDrop. To avoid differences in terminal restriction

fragment (T-RF) profiles due to variation in the amount of loading DNA (Fredriksson et al. 2014), the purified amplicons of 200 ng bacterial and archaeal 16S rDNA were digested with *Msp*I and *Hha*I (Moeseneder et al. 2001) restriction enzymes, respectively. Terminal restriction fragment length polymorphism (T-RFLP) analysis was conducted by Macrogen.

2.7. Cloning, sequencing and phylogenetic analysis

To construct 16S rRNA libraries, the RNA of selected SIP fractions and the Day 0-slurry were reverse transcribed into cDNA using 907R and 958R primers, as above. The bacterial and archaeal 16S rRNAs were amplified using the 8F/907R and 21F/958R primer sets and purified using a PCRquick-spin™ PCR purification kit. PCR amplicons were cloned with a pGEM-T Easy Vector kit according to the manufacturer's instructions (Promega). Sequencing was conducted by SolGent. All sequences were checked for chimeric artefacts using the chimera slayers in the MOTHUR program (Schloss et al. 2009) and aligned with closely related sequences obtained from the GenBank databases using the ClustalW in MEGA4 software. Sequences that were ≥97% similar were grouped as the same bacterial and archaeal phylotypes. Rarefaction curves were calculated using the MOTHUR program (Fig. S3). Phylogenetic tree inference was constructed using the neighbor-joining method with the Jukes and Cantor distance model implemented within the software package MEGA4. Node support was assessed by bootstrapping with 1000 bootstrap replicates. The length of respective T-RFs was identified on the sequence of clones. Sequence data were submitted to GenBank under accession numbers MK108080–MK108100 (partial bacterial 16S rRNA sequences in the heavy fraction), MK110379–MK110419 (partial sequences of the bacterial 16S rRNA at EB1), MK110425–MK110475 (partial sequences of the bacterial 16S rRNA at EB6) and MK120362–MK120424 (partial sequences of the archaeal 16S rRNA).

3. RESULTS

3.1. Environmental parameters and metabolic rate measurements

The total C_{org} content in the surface sediment was 2.7 and 2.5% at EB1 and EB6, respectively (Table 1).

Table 1. Environmental settings and surface sediment (0–3 cm depth) characteristics at the sampling sites on the continental shelf (EB1) and center (EB6) of the Ulleung Basin

Environmental parameters	EB1	EB6
Location	37° 00′ N, 129° 30′ E	37° 00′ N, 131° 30′ E
Water depth (m)	135	2159
Sediment temperature (°C)	2.3	0.2
Porosity	0.7	0.9
Total organic carbon (%; dry wt.)	2.72	2.49
Total nitrogen (%; dry wt.)	0.41	0.41

At EB6, depth distributions of Fe^{2+} and Mn^{2+} in pore-water, total $Mn_{(DCA)}$, $Fe(III)_{(oxal)}$ and $Fe(II)_{(oxal)}$ in solids and SRRs indicated approximate zones of MnR (Mn^{2+} accumulation and $Mn_{(DCA)}$ depletion) at 0–3 cm and Fe reduction (Fe^{2+} and $Fe(II)_{(oxal)}$ accumulation and $Fe(III)_{(oxal)}$ depletion) at 3–6 cm, while SRR was suppressed to ≥6 cm (Fig. 2, Table 2). At EB1, MnR was not indicated, while Fe^{2+} and $Fe(II)_{(oxal)}$ accumulation indicated Fe reduction at 0–4 cm and SRR reached a plateau below 4 cm depth. Concentrations of NO_x were only above background levels in the surface layers (0–2 cm) at both sites while NH_4^+ concentrations were similar across depths and sites (Table 2).

Depth-integrated (0–6 cm) anaerobic C_{org} oxidation rates were 5.11 and 7.86 mmol m^{-2} d^{-1} at EB1 and EB6, respectively (Table 3), and overall the partitioning between TEAPs agreed well with the redox zonation inferred from the pore-water and solids. SR dominated as the TEAP at EB1, sustaining 65% of C_{org} oxidation while dissimilatory FeR accounted for 25%. FeR was concentrated at 2–4 cm depth, comprising 57% of anaerobic C_{org} oxidation (1.15 mmol C m^{-2} d^{-1}; Table 3, Fig. 2). In contrast, at EB6, FeR was not discernible at 0–2 cm depth but the FeRR increased with depth; FeR attained dominance, contributing more than 90% of anaerobic C_{org} oxidation, at 4–6 cm depth (2.71 mmol C m^{-2} d^{-1}). The SRR within the upper 6 cm depth of EB6 ranged from 0.1–0.2 mmol C m^{-2} d^{-1} and contributed less than 10% of C_{org} oxidation at all depths.

3.2. Slurry incubations amended with acetate

DIC concentrations increased with time in all slurry incubations, and DIC accumulation was further stimulated by the addition of acetate, with an immediate effect at EB6 and an apparent lag phase of 3 d at EB1

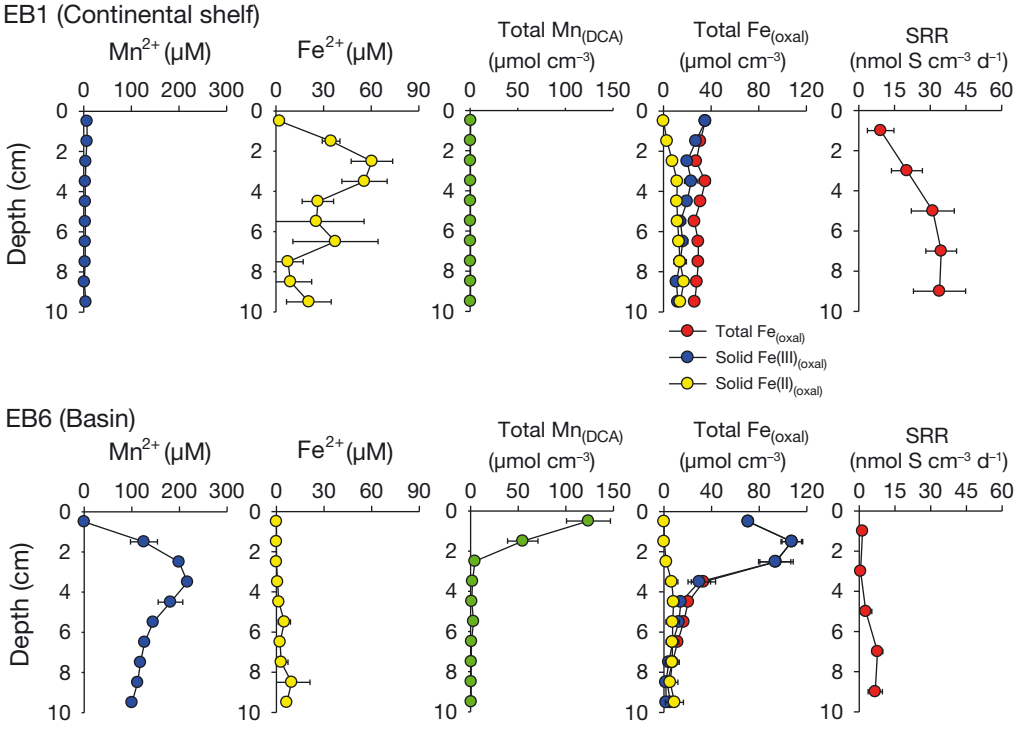

Fig. 2. Vertical distributions of the geochemical constituents Mn^{2+} and Fe^{2+} in the pore-water, solid-phase manganese (total $Mn_{(DCA)}$), solid-phase iron (total $Fe_{(oxal)}$, $Fe(III)_{(oxal)}$ and $Fe(II)_{(oxal)}$) and rates of sulfate reduction at the sediments of sites EB1 and EB6 (see Fig. 1 for site locations). SRR: sulfate reduction rate. Depth profiles of Mn^{2+} and total $Mn_{(DCA)}$ at EB1 were re-drawn from Na et al. (2018)

Table 2. Depth-integrated inventories of the pore-water and solid-phase constituents in the continental shelf (EB1) and center (EB6) of the Ulleung Basin. $Mn_{(DCA)}$: dithionite-citrate-acetic acid-extractable Mn; $Fe_{(oxal)}$: oxalate-extractable Fe

Station	Depth interval (cm)	Pore-water (mmol m^{-2})				Solid phase (mmol m^{-2})			
		NH_4^+	NO_x	Mn^{2+}	Fe^{2+}	Total $Mn_{(DCA)}$	Total $Fe_{(oxal)}$	$Fe(III)_{(oxal)}$	$Fe(II)_{(oxal)}$
EB1 (Continental shelf)	0–2	1.06	0.033	0.09	0.24	11.3	661	630	31
	2–4	1.27	0.003	0.06	0.85	9.2	626	435	191
	4–6	1.07	0.003	0.04	0.34	8.9	571	340	231
	Sum (0–6)	3.40	0.039	0.19	1.43	29.4	1858	1405	453
EB6 (Basin)	0–2	1.15	0.023	1.08	0.00	1786	1784	1782	3
	2–4	1.15	0.005	3.55	0.01	67.6	1273	1233	85.6
	4–6	1.14	0.004	2.65	0.05	44.6	370	269	155
	Sum (0–6)	3.44	0.032	7.28	0.06	1898	3427	3284	244

(Fig. 3a,b). Acetate concentrations in the control slurries stayed below 25 μM (Fig. 3c,d), whereas acetate accumulated in the slurries amended with ^{12}C- and ^{13}C-acetate from time zero to Day 3 (EB6) or Day 5 (EB1), whereafter the concentration decreased to levels similar to the controls, with the decrease being abrupt at EB6 and more gradual towards the end of incubation (Day 17) at EB1.

Dissolved Mn^{2+} concentrations in all slurries of EB1 remained extremely low (<21 μM) during the course of the incubation, indicating that no MnR occurred (Fig. 3e), whereas Mn^{2+} at EB6 showed steep increases throughout the incubation in the slurries amended with acetate (Fig. 3f). Dissolved Fe^{2+} accumulated during the first 7 d of incubation at EB1, with 2.4 times higher rates in the acetate-amended slurries than in the control (Fig. 3g), whereas the Fe^{2+} concentrations stayed below the detection limit throughout the incubation in all slurries of EB6 (Fig. 3h). Sulfide concentrations remained low (<12 μM) at EB1 and stayed below the detection limit at EB6 (data not shown).

3.3. Microbial communities in the surface sediments

The T-RFLP profiles of reversely transcribed and amplified bacterial 16S rRNA from the freshly collected sediment showed diverse metabolically active

Table 3. Depth-integrated microbial iron and sulfate reduction in rates of carbon oxidation (mmol C m^{-2} d^{-1}): carbon mineralization by microbial Fe(III) reduction: $8FeOOH + CH_3COO^- + 8H^+ = 2HCO_3^- + 8Fe^{2+} + 12H_2O$; organic carbon ($C_{org}$) oxidation by sulfate reduction: $SO_4^{2-} + CH_3COO^- + 2H^+ = 2HCO_3^- + HS^-$. Numbers in parenthesis: relative contribution (%) of microbial Fe and sulfate reduction to total anaerobic C respiration, respectively. Note that because iron (FeRR) and sulfate reduction rates (SRR) and C_{org} oxidation were determined independently, the summed contribution of FeRR and SRR can exceed 100% of C_{org} oxidation as a result of the uncertainty associated with each method. nd: not detected

Site	Depth interval (cm)	Anaerobic C oxidation	Microbial Fe reduction[a]	SO_4^{2-} reduction
EB1	0–2	1.78	0.11 (6.1)	0.85 (47.7)
	2–4	2.04	1.15 (56.6)	1.28 (62.6)
	4–6	1.28	nd	1.19 (92.6)
	Sum (0–6 cm)	5.11	1.26 (24.7)	3.32 (65.0)
EB6	0–2	2.99	nd	0.14 (4.6)
	2–4	2.14	0.16 (7.5)	0.11 (5.0)
	4–6	2.74	2.71 (99.4)	0.2 (7.2)
	Sum (0–6 cm)	7.86	2.88 (36.6)	0.44 (5.6)

[a]Stoichiometric equations were used to estimate microbial Fe(III) reduction; abiotic reduction of Fe(III) by sulfide oxidation: $3H_2S + 2FeOOH = 2FeS + S^0 + 4H_2O$; microbial Fe(III) reduction = total Fe(III) reduction − abiotic Fe(III) reduction

bacterial communities at both the continental shelf (EB1) and the center of the basin (EB6) (Fig. 4), whereas the profiles for archaea were completely dominated by a single fragment length at both sites (Fig. S4). Based on the derived clone libraries, the bacterial community in the sediment of EB1 was dominated by *Gammaproteobacteria* and *Deltaproteobacteria*, accounting for 41 and 30% of the total bacterial 16S rRNA sequences, respectively (Table 4). Most *Gammaproteobacteria* were affiliated with clones previously detected in methane or hydrocarbon seep sediments (Beal et al. 2009, Redmond et al. 2010, Ruff et al. 2013) and several deep-sea sediments (Li et al. 1999, Schauer et al. 2010, 2011) (Fig. S5). In the deltaproteobacterial group, most sequences were classified as *Desulfobacteraceae*, a family known primarily as sulfate reducers, representing 22% of all bacterial clones (16 sequences). Only 2 sequences affiliated with *Desulfuromonadales* and 2 sequences within the *Myxoccoccaceae* were detected (Fig. S6).

At EB6, *Gammaproteobacteria* constituted 38% of total bacterial 16S rRNA sequences, very similar to EB1, while the contribution of *Deltaproteobacteria* was reduced to 12% and that of *Alphaproteobacteria* increased to 12% (Table 4). In the *Gammaproteobacteria*, 4 sequences in the *Colwelliaceae* family were observed at the beginning of the incubation, and 7 sequences were closely affiliated with the genus *Thioalkalivibrio* (91.8% similarity) known as a chemolithoautotrophic sulfur-oxidizer (Fig. S5). Among the *Deltaproteobacteria*, only 2 sequences belonged to the *Desulfobacteraceae* (Fig. S6). Four deltaproteobacterial sequences were not affiliated with known deltaproteobacterial isolates but clustered with a putative acetate-oxidizing Mn-reducer (JN621407) of the UB sediment (Vandieken & Thamdrup 2013) (Fig. S6). Only 2 sequences were affiliated with the *Desulfuromonadales*. Most of the alphaproteobacterial sequences fell into the family *Rhodospirillaceae*. Phylotypes affiliated with the *Bacteroidetes*, *Chloroflexi*, *Planctomycetes* and *Verrucomicrobia* were also observed as minor bacterial groups in the sediments of both sites, but *Betaproteobacteria* were only detected at EB1, whereas *Acidobacteria*, *Actinobacteria* and *Nitrospira* were only retrieved at EB6.

Among the total of 102 archaeal 16S rRNA sequences, *Thaumarchaeota* predominated at both sites, comprising approximately 80% of the total archaeal sequences at each site (Table 4). The operational taxonomic units (OTUs) within the *Thaumarchaeota* at EB6 (14 phylotypes) appeared more phylogenetically diverse than those at EB1 (2 phylotypes), and *Thaumarchaeota* at EB6 were not clustered with the thaumarchaeotal sequences of EB1 (Fig. S7), indicating that the community composition of *Thaumarchaeota* inhabiting in the continental shelf and basin varies with geographical distance or biogeochemical condition. Sequences affiliated with the Marine Benthic Group B (MBGB; Vetriani et al. 1999, also known as the Deep-Sea Archaeal Group or *Lokiarchaeota*; Spang et al. 2015) comprised 17% of the total archaeal 16S rRNA sequences in the sediment from EB1 whereas only one MBGB sequence was detected in the sediment from EB6 (Table 4, Fig. S8).

3.4. ^{13}C-labeled microbial groups revealed by RNA-SIP

At EB1, a small T-RF peak at 474 bp obtained with the restriction enzyme *Msp*I and observed in the original sediment and in the control slurry at Day 7 increased prominently in all acetate-amended slur-

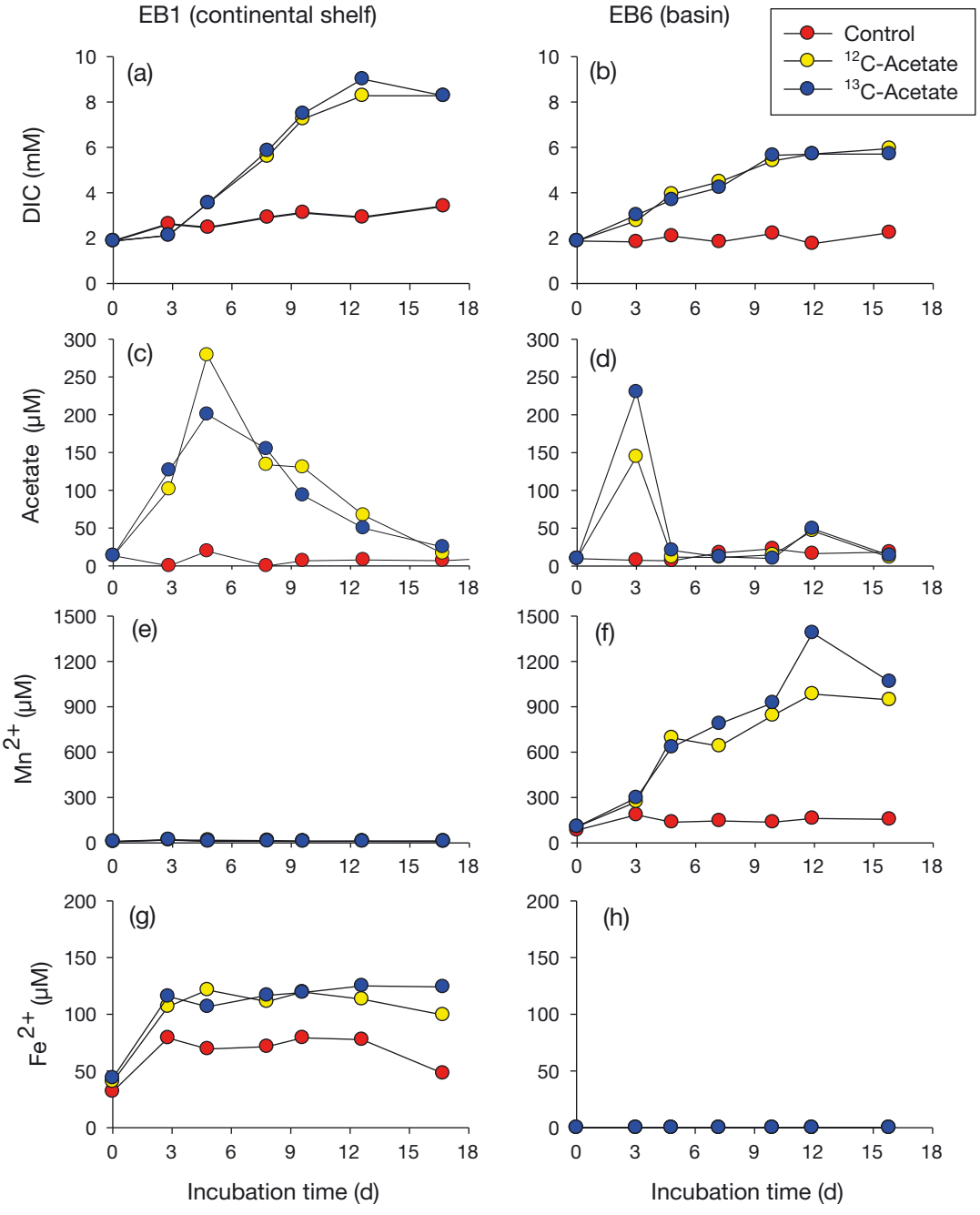

Fig. 3. Change in concentrations of dissolved inorganic carbon (DIC), acetate, Mn^{2+} and Fe^{2+} during anoxic incubations of sediment slurries at sites EB1 and EB6 (see Fig. 1 for site locations)

ries (Fig. 4). This result suggests that one bacterial group was actively stimulated well beyond its activity in the control with the addition of acetate, incorporating acetate carbon into their RNA. At EB6, 4 major peaks occurring at 83, 474, 494 and 498 bp in the heavy SIP fraction of the ^{13}C-acetate incubations indicated bacterial groups that were presumably responsible for the oxidation of the added acetate. These 4 peaks were also present in the original sediment and changed less in the light fraction than was the case for the 474 bp peak at EB1. This result, together with the immediate stimulation of acetate oxidation after the amendment at EB6 (Fig. 3), suggests that more diverse bacterial groups play a role

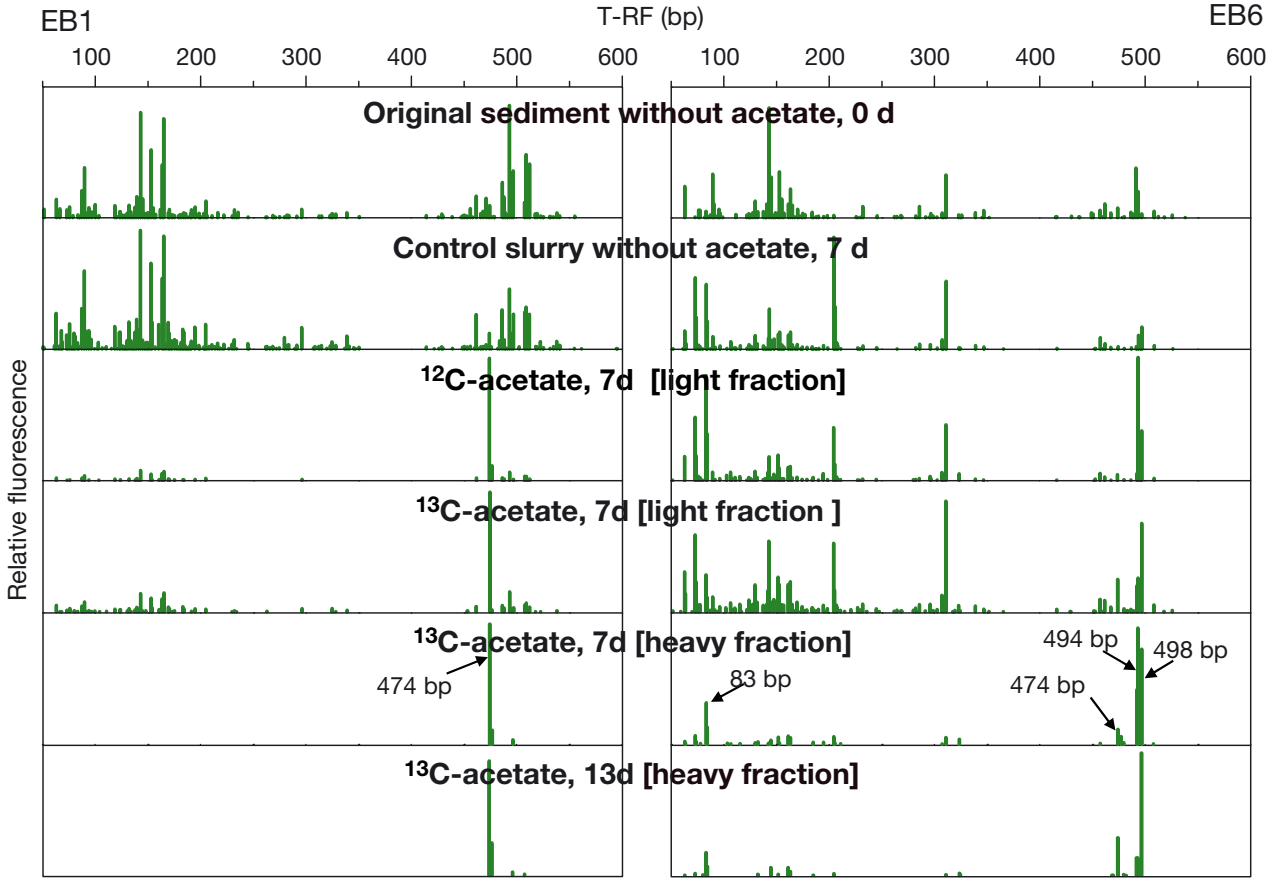

Fig. 4. Terminal restriction fragment length polymorphism analyses (*Msp*I) of bacterial 16S rRNA-cDNA amplicons obtained from one selected heavy and light fraction of incubations with ^{13}C-acetate amendment of EB1 and EB6 sediment slurries in comparison with the original sediment and selected light fractions of incubation with ^{12}C-acetate

as acetate-oxidizers in sediment slurries from EB6 than those from EB1, and that these groups were already relatively active *in situ*, although a true 1-to-1 relationship between T-RFLP peaks and phyletic clades cannot be expected.

The clone libraries of reversely transcribed bacterial 16S rRNA from one heavy fraction of the ^{13}C-acetate-amended incubation from EB1 revealed that all sequences (total: 50 sequences) belonged to the genus *Arcobacter* in the *Epsilonproteobacteria* (Fig. 5). The 16S rRNA sequences of *Arcobacter* represented a T-RF with 474 bp (Fig. 4). The most abundant *Arcobacter* sequences (OTU SIP-B31, 72% of clones) almost coincided with a putative Mn-reducing acetate-oxidizer (JQ863497, similarity of 99.8%) detected from coastal sediment in Aarhus Bay, Denmark (Vandieken & Thamdrup 2013). On the other hand, sulfate-reducing bacteria (SRB) of the *Deltaproteobacteria* were not identified in the heavy RNA-SIP fraction of the ^{13}C-acetate-amended incubation of the EB1 sediment. At EB6, the library from the ^{13}C-acetate-amended incubation was dominated by sequences associated with 3 clades: *Alteromonadales* and *Oceanospirillales* in *Gammaproteobacteria* and *Desulfuromonadales* in *Deltaproteobacteria* (Fig. 5). Most 16S rRNA gene sequences in *Alteromonadales* and *Oceanospirillales* will be restricted at 494 bp by *Msp*I, and a few sequences in these clades make T-RFs of 496 and 498 bp length. *Desulfuromonadales* 16S rRNA sequences are predicted to make T-RFs of multiple lengths (131, 164 and 511 bp). One sequence belonging to *Fusobacteria* was retrieved as a minor ^{13}C-labeled bacterial group. By contrast, members of *Arcobacter* were not present in the 16S rRNA library of the heavy fraction of EB6.

The T-RFLP profiles of archaeal 16S rRNA showed only one dominant T-RF (326 bp length) in both the original sediments and in all incubated slurries from both sites (Fig. S4). The majority of ^{13}C-labeled archaeal 16S rRNA sequences detected in the heavy

Table 4. Phylogenetic affiliation of bacterial and archaeal 16S rRNA sequences obtained from clone libraries from the beginning of incubation (Day 0), and heavy stable isotope probing (SIP) fractions (Day 7) from incubations of sediment from the continental shelf (EB1) and basin (EB6) of the Ulleung Basin. Numbers in parentheses: relative abundance of each phylogenetic group; (–) not detected; MCG: Miscellaneous Crenarchaeotal Group; MBGB: Marine Benthic Group B; MBGD: Marine Benthic Group D

Phylogenetic affiliation	EB1 0–3 cm		EB6 0–3 cm	
	Day 0	Heavy fraction	Day 0	Heavy fraction
Bacteria				
Actinobacteria	–	–	1 (1.3)	–
Acidobacteria	–	–	4 (5.2)	–
Bacteriodetes	3 (4.1)	–	2 (2.6)	–
Chloroflexi	1 (1.4)	–	2 (2.6)	–
Fusobacter	–	–	–	1 (2.4)
Nitrospira	–	–	2 (2.6)	–
Alphaproteobacteria	–	–	9 (11.7)	–
Betaproteobacteria	1 (1.4)	–	–	–
Deltaproteobacteria	22 (29.7)	–	9 (11.7)	4 (9.8)
Gammaproteobacteria	30 (40.5)	–	29 (37.7)	32 (78.0)
Epsilonproteobacteria	–	50 (100)	–	–
Planctomycetes	1 (1.4)	–	2 (2.6)	–
Verrucomicrobia	2 (2.7)	–	1 (1.3)	–
Unclassified	14 (18.9)	–	16 (20.8)	4 (9.8)
Good's coverage (%)[a]	27	86	13	65
Total number of clones	74	50	77	41
Archaea				
Thaumarchaeota	42 (77.8)	15 (48.4)	40 (83.0)	18 (60.0)
MCG	2 (3.7)	4 (12.9)	1 (2.1)	2 (6.7)
MBGB	9 (16.7)	9 (21.6)	1 (2.1)	2 (6.7)
MBGD	1 (1.9)	2 (6.5)	4 (8.3)	4 (13.3)
Unclassified	–	1 (2.0)	2 (4.2)	4 (13.3)
Good's coverage (%)[a]	76	61	50	46
Total number of clones	54	31	48	30

[a]Good's coverage (%) = [1 – (n / N)] × 100, where n = number of operational taxonomic units; N = total number of clones

fraction from the ^{13}C-acetate-amended slurries of EB1 (48% of the total archaeal sequences, n = 15) belonged to the thaumarchaeotal group, 22% grouped within the MBGB, 13% within the Miscellaneous Crenarchaeotal Group (MCG; Inagaki et al. 2003, also known as *Bathyarchaeota*; Meng et al. 2014) and 6.5% within the Marine Benthic Group D (MBGD; Vetriani et al. 1999) (Table 4). MBGB and MBGD archaeal groups in EB1 are predicted to make T-RFs of 352 and 327 bp, respectively, and the T-RFs of MCG might appear in various sizes because MCG archaeal sequences have a different restriction site on their 16S rRNA gene, but the T-RFs of these archaeal groups were not seen in the results of the T-RFLP analysis (Fig. S4). All ^{13}C-labeled thaumarchaeotal sequences of EB1 belonged to the OTU SIP-A14 (Fig. S7). Meanwhile, more diverse thaumarchaeotal OTUs were detected among the ^{13}C-labeled archaeal 16S rRNA sequences from EB6 (60%, n = 18). Additionally, 4 sequences belonged to the MBGD, 2 sequences to the MCG and 2 sequences to the MBGB group (Table 4, Fig. S8). The ^{13}C-labeled MBGD archaea in EB6 have a different *Hha*I restriction site on the 16S rRNA gene than the MBGD in EB1, yielding a T-RF length of 197 bp. From the T-RFLP analysis, the T-RF of *Thaumarchaeota* in the heavy fraction of the acetate-amended slurry was still the sole dominant peak after 13 d (Fig. S4). No reverse transcript real-time PCR products of archaeal 16S rRNA were obtained from the heavy SIP-fractions of ^{12}C-acetate or the non-amended control incubations (Table S1).

4. DISCUSSION

4.1. Major anaerobic C_{org} oxidation pathways and associated microbial communities

We observed distinct differences in the partitioning of TEAPs between the continental shelf (EB1) and the basin floor (EB6). At EB1, SR appeared the predominant C_{org} oxidation pathway at 0–6 cm, comprising 65% of the total anaerobic C_{org} oxidation while microbial FeR contributed 25% (Table 3). The remaining 10% of C_{org} oxidation might be associated with denitrification (Table 3; cf. Na et al. 2018). Based on the low total $Mn_{(DCA)}$ content and lack of Mn^{2+} accumulation in porewater (Table 2, Fig. 2), dissimilatory MnR was not suggested to be significant in the sediment at EB1. Overall, these results indicate that various bacterial groups using NO_3^-, iron oxide and sulfate as the sole terminal electron acceptor are sequentially responsible for C_{org} oxidation in surface sediment of the continental shelf (EB1). High rates of SR at EB1 were reported previously (Hyun et al. 2010), and our results confirm that this process indeed accounts for a large fraction of C_{org} oxidation, as often observed in shelf sediments (Canfield et al. 2005, Jørgensen & Kasten 2006).

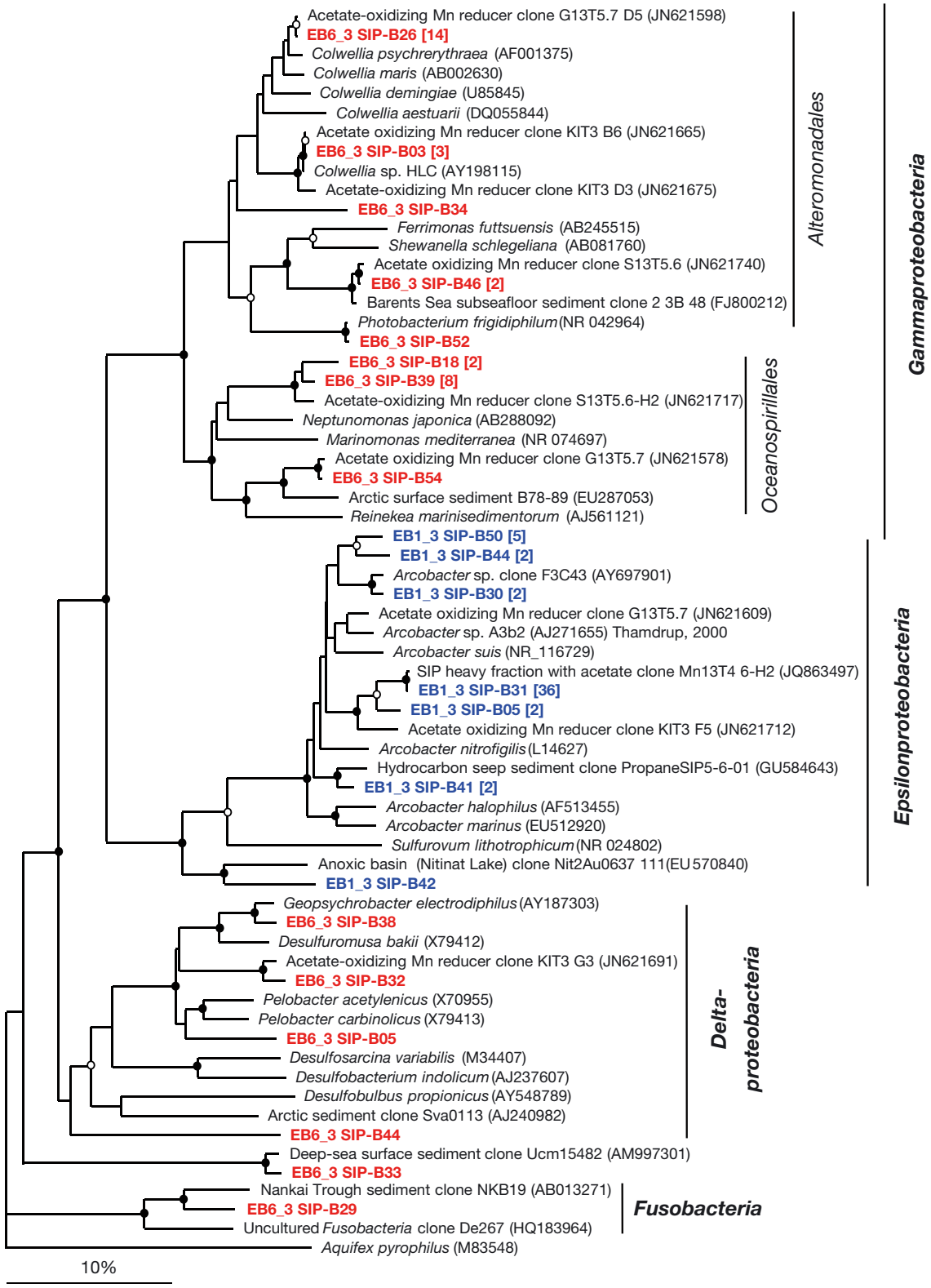

Fig. 5. Bacterial 16S rRNA-cDNA phylogenetic tree showing the affiliation of operational taxonomic units detected in one heavy fraction of the ^{13}C-acetate-amended incubation from sites EB1 and EB6. Bootstrap value intervals are indicated as blank circles (75–90%) and black circles (>90%). Sequences retrieved in this study are highlighted in **bold**. Scale bar: 10% estimated sequence divergence

In contrast to EB1, C_{org} oxidation by SR contributed only 5.6% of total anaerobic C_{org} oxidation in the surface sediment (0–6 cm depth) of the basin of UB (EB6). Instead, based on the abundance of manganese oxide and accumulation of Mn^{2+} in porewater (Table 2), MnR was indicated to be the predominant C_{org} oxidation pathway at 0–6 cm depth, contributing approximately 50% of total anaerobic C_{org} oxidation, which agrees well with the results of Hyun et al. (2017) that MnR accounted for 57% of anaerobic C_{org} in center of the UB basin. MnR was the overwhelming anaerobic C_{org} oxidation pathway (>90% of total anaerobic C_{org} oxidation) to 4 cm depth, while microbial FeR accounted for 99% of the total anaerobic C_{org} oxidation at 4–6 cm depth (Table 3). Thus, SR in the basin is presumably suppressed by competition from Mn- and Fe-reducing bacteria (Hyun et al. 2010, 2017).

In accordance with the dominance of the SR in C_{org} oxidation at EB1, the clone library of reversely transcribed bacterial 16S rRNA at 0–3 cm depth of the continental shelf (EB1) revealed a large fraction of deltaproteobacterial sequences belonging to *Desulfobacteraceae* (22% of the total bacterial 16S rRNA sequences), which was previously reported as an important SRB group in various marine sediments (Leloup et al. 2009, Zeleke et al. 2013). In contrast to EB1, and corresponding to the relatively low SRR, only 2 deltaproteobacterial sequences were affiliated with SRB at EB6 (Fig. S6). Instead, many bacterial sequences were related to putative Mn-reducing groups in the *Gammaproteobacteria*, such as *Colwelliaceae* and *Shewanellaceae* in the order *Alteromonadales* and *Oceanospirillaceae* in the order *Oceanospirillales* (Fredrickson et al. 2008, Vandieken et al. 2012, Vandieken & Thamdrup 2013). Thus, the structure and function of the microbial communities in the surface sediment of the UB are directly controlled by the quantity and quality of the organic matter derived from the water column (Danovaro et al. 2000, Probandt et al. 2017) and the presence of available electron acceptors (Orcutt et al. 2011, Vandieken & Thamdrup 2013).

4.2. Acetate-oxidizing bacteria

The DIC accumulation and the acetate depletion to *in situ* levels in the acetate-amended slurries indicate the presence of an active acetate-oxidizing microbial community. Based on the diverse C_{org} oxidation pathways taking place at EB1 (Table 3), we first anticipated that acetate-oxidizing bacterial groups using iron oxide or sulfate as electron acceptors would be labeled with ^{13}C from added acetate during the incubation of the EB1 sediment slurry. The increase in dissolved iron (Fe^{2+}) and solid-phase $Fe(II)_{(oxal)}$ in acetate-amended slurries relative to the control (Figs. 3g & S9A) indicated that acetate oxidation in the acetate-amended slurries was at least in part related to FeR. Indeed, the concentration of $Fe(III)_{(oxal)}$ was sufficient to facilitate dissimilatory FeR in the slurry throughout the incubation (>17 µmol cm^{-3}; Fig. S9B). Despite the continuous accumulation of $Fe(II)_{(oxal)}$, the soluble Fe^{2+} concentrations only increased steeply during the first 3 d of incubation (Fig. 3g). Although we did not measure the contribution of SR to DIC production during the slurry incubation, it is likely that the process was active, as in the original sediment (Fig. 2). Thus, sulfide produced by SR might react with Fe^{2+} to precipitate FeS. In addition to Fe- and sulfate reducers, nitrate reducers could also incorporate ^{13}C initially, but the nitrate pool of the sediment would be rapidly depleted in the anoxic slurries and its contribution to acetate oxidation through the experiment would be miniscule. However, repetitive addition of acetate led almost exclusively to ^{13}C-labeling of members of *Arcobacter* that were not retrieved in the 16S rRNA library in the original sediment (Table 4, Fig. 3). The complete dominance of *Arcobacter* in the heavy fraction is a strong indication that this group directly assimilated the added ^{13}C-acetate during the incubation rather than, e.g. cross-feeding autotrophically on ^{13}C-DIC. Indeed, several uncultured members of *Arcobacter* were already reported as important acetate-oxidizers in several incubation experiments amended with acetate (Webster et al. 2010, Vandieken et al. 2012, Vandieken & Thamdrup 2013) and seawater (Berg et al. 2013). Thus, the *Arcobacter* detected in this study might be considered as a significant acetate-oxidizing bacterial group in the slurry of EB1. RNA-SIP studies previously indicated members of *Arcobacter* as important acetate-oxidizers in marine sediments, utilizing oxygen, nitrate and manganese oxide as electron acceptors (Vandieken et al. 2012, Vandieken & Thamdrup 2013). In earlier studies in Black Sea shelf sediment, Thamdrup et al. (2000) also reported abundant *Arcobacter*-related microorganisms in most probable number (MPN) dilutions with acetate as the sole carbon source and manganese oxide as an electron acceptor, further indicating their ecological significance in manganese oxide-rich sediment. However, although the ^{13}C-labeled *Arcobacter* OTU (OTU EB1_3 SIP-B31) in our slurry experiment was >99% phylogenetically similar to those retrieved in

the previous RNA-SIP sediment studies (Vandieken et al. 2012, Vandieken & Thamdrup 2013), the anoxic condition, rapid depletion of nitrate and lack of dissolved Mn^{2+} accumulation both during the course of the incubation experiment and in the sediment profile (Figs. 2 & 3e) suggests that neither oxygen, nitrate nor Mn was important for acetate oxidation in EB1, and thereby for the labeling of *Arcobacter* in our experiment. While dissimilatory reduction of Fe oxide or sulfate has not been observed in *Arcobacter*, a strain of *A. anaerophilus* isolated from corrosion enrichments has been shown to grow on both acetate and complex organic substrates as an electron donor and ferric iron citrate or elemental sulfur as an electron acceptor (Roalkvam et al. 2015) and strains of the same species were isolated from estuarine sediment (Sasi Jyothsna et al. 2013). Thus, potential explanations for our RNA-SIP result could be either that *Arcobacter* in our experiments possessed the ability to reduce solid Fe(III) species or that they, like *A. anaerophilus*, coupled acetate oxidation to elemental sulfur reduction with sulfur being regenerated through abiotic re-oxidation of sulfide by the sedimentary Fe(III) oxide pool (Yao & Millero 1996).

Interestingly, no incorporation of ^{13}C-acetate into known SRB was detected in slurries of surface sediments (0–3 cm depth), although the SRR was high in the whole intact cores at EB1 (Table 3). In addition, from the T-RFLP analysis, the T-RFs of other bacteria (except for *Arcobacter*'s T-RF) were almost invisible in the heavy fraction after 13 d of the incubation (Fig. 4). This result corresponds with previous studies (Webster et al. 2010, Vandieken et al. 2012, Vandieken & Thamdrup 2013), suggesting that sulfate reducers have a relatively slow turnover of their ribosomal RNA (Vandieken & Thamdrup 2013) or they might be less successful in the competition for the added substrate compared to other acetate-oxidizing bacteria, such as Mn-, Fe- and nitrate reducers (Sørensen 1982, Achtnich et al. 1995). Alternatively, acetate may not be the preferred C_{org} source for sulfate reducers in the sediments of EB1.

In contrast to EB1, more diverse microbial groups were responsible for the oxidation of acetate at EB6. Bacteria affiliated with *Colwellia* and *Oceanospirillaceae* were identified as important acetate-oxidizing Mn reducers in the slurry (Fig. 5). The most abundant bacterial sequences have a high similarity (99.8%) to an OTU within *Colwellia*, which was indicated by RNA-SIP as a dominant acetate-oxidizing Mn-reducer in 3 sediments from the Ulleung Basin, Gullmar Fjord and Aarhus Bay (Vandieken et al. 2012, Vandieken & Thamdrup 2013). No *Arcobacter* affiliates were detected in the ^{13}C-heavy fraction 16S rRNA library, even though a T-RF predicted as *Arcobacter* could be observed as a minor peak in the original sediment and heavy fraction of ^{13}C-acetate (Fig. 4). This result indicates that members of *Arcobacter* contribute less to Mn and acetate turnover than other bacteria in the sediment of EB6.

4.3. *Thaumarchaeota* labeled with ^{13}C in anoxic condition

Transcribed archaeal 16S rRNA T-RFLP analysis revealed that archaeal RNA was labeled with ^{13}C during the incubation with ^{13}C-acetate, which was also supported by a general absence or background level of reverse transcript real-time PCR products of archaeal 16S rRNA from the heavy SIP-fractions of ^{12}C-acetate and the non-amended control incubations (Table S1). The increase in archaeal 16S rRNA copy numbers in the ^{13}C-labeled fraction of the ^{13}C-acetate-amended slurries after 7–13 d (Table S1) suggests that some active archaeal groups actively incorporated carbon from added acetate under anoxic conditions. Most archaeal 16S rRNA sequences labeled with ^{13}C belonged to *Thaumarchaeota*. These *Thaumarchaeota* labeled in the UB sediment might either be autotrophs using the ^{13}C-DIC produced by ^{13}C-acetate-oxidizing bacteria or be able to assimilate acetate heterotrophically as a carbon source. Most ^{13}C-labeled *Thaumarchaeota* 16S rRNA sequences fell into the alpha clade (Durbin & Teske 2010) that has been retrieved in surface sediment and the water column and their closest isolate is *Nitrosopumilus maritimus* (similarity 97%; Fig. S7) (Könneke et al. 2005), which is an ammonia-oxidizing chemolithoautotroph. *Thaumarchaeota* are considered important ammonia-oxidizing autotrophs in marine environments (Francis et al. 2005, Wuchter et al. 2006, Gillan & Danis 2007), especially in low-oxygen environments such as marine sediment and oxygen-minimum zone waters (Agogué et al. 2008, Park et al. 2008, Jin et al. 2011). Although *Thaumarchaeota* in such environments may be adapted to low oxygen levels (Bristow et al. 2016), their pathway of ammonium oxidation is strictly aerobic (e.g. Lancaster et al. 2018) and should hence be inhibited in our anoxic slurries.

Alternatively, the ^{13}C-labeled *Thaumarchaeota* may have assimilated ^{13}C-labeled acetate. The growth of some thaumarchaeotal members using various organics (amino acid, urea and organic acids)

has been reported in many previous studies (Ouverney & Fuhrman 2000, Teira et al. 2006, Alonso-Sáez et al. 2012, Qin et al. 2014). Additionally, some thaumarchaeotal members from salt marsh sediments can utilize various organic compounds such as acetate, glycine or urea, lipids and proteins, but they do not use bicarbonate as a carbon source (Seyler et al. 2014). Although direct evidence on the mechanisms of C_{org} assimilation by *Thaumarchaeota* has not been reported yet (Kim 2015), a heterotrophic lifestyle of some members of *Thaumarchaeota* in organic-rich marine sediment cannot be excluded, though their energy metabolism requires further elucidation.

5. CONCLUSIONS

The composition of the microbial communities and acetate-utilizing microbial groups differed distinctly between the 2 geochemically contrasting sediments in the shelf and basin center of the UB. In the continental shelf (EB1), where anaerobic C_{org} oxidation was dominated by SR and FeR, uncultured SRB in *Desulfobacteraceae*, accounting for 22% in the total bacterial 16S rRNA sequences, are likely to contribute a significant part of the anaerobic C_{org} oxidation. However, SRB were not detected as acetate-oxidizers among the ^{13}C-labeled bacteria during the anoxic slurry incubation. Instead, *Arcobacter*-related bacteria were proposed as a major acetate-oxidizing clade, coupled either directly to FeR or indirectly to reduction of elemental sulfur produced via re-oxidation of sulfur by Fe(III). Meanwhile, bacteria related to *Colwelliaceae*, *Shewanellaceae* and *Oceanospirillaceae* were identified as putative Mn-reducing bacteria, accounting for 8% of clones in *Bacteria* at the Mn-rich site EB6 at the center of the basin. Similarly, the bacterial members affiliated with *Colwellia* and *Oceanospirillales* were retrieved as major acetate-oxidizing bacterial groups associated with MnR at EB6. Interestingly, ^{13}C-labeling of *Thaumarchaeota* under anoxia suggests that this group may take up either C_{org} (acetate) or inorganic carbon during anaerobic metabolism in the sediments of the UB. Our findings, using RNA-SIP in combination with biogeochemical analyses, thus provide intriguing information on the ecological and biogeochemical role of the members of *Arcobacter* as Fe-reducers and the *Thaumarchaeota* possessing metabolic activities in anoxic conditions in the sediments of UB. Given that the benthic microbial communities related to C_{org} oxidation are influenced by quantitative and qualitative changes in organic matter together with the availability of electron acceptors, our results provide relevant ecological baseline information on the response of benthic microbial ecosystems to ongoing climate change in the UB.

Acknowledgements. We thank the captain and crew of the RV 'Eardo' of the KIOST for their help during the cruise. We thank Dr. Hannah Sophia Weber (University of Southern Denmark) for technical support with ultracentrifugation for the fractionation of labeled RNA. Biogeochemical analysis and metabolic rate measurements were supported by the research programs titled 'Korea-Long-Term Marine Ecological Research (K-LTMER)' and 'Deep Water Circulation and Material Cycling in the East Sea' funded by the Korean Ministry of Oceans and Fisheries. Analysis for microbial communities was supported by the Mid-career Researcher Program funded by the Korean Ministry of Science and ICT (No. 2018R1A2B2006340). Microbiological analysis for RNA-SIP was conducted as an international collaborative research program supported by the National Research Foundation of Korea (NRF-2012-013-2012S1A2A1A01030760) and the Danish Council for Independent Research and the Danish National Research Foundation (DNRF53).

LITERATURE CITED

Achtnich C, Bak F, Conrad R (1995) Competition for electron donors among nitrate reducers, ferric iron reducers, sulfate reducers, and methanogens in anoxic paddy soil. Biol Fertil Soils 19:65–72

Agogué H, Brink M, Dinasquet J, Herndl G (2008) Major gradients in putatively nitrifying and non-nitrifying archaea in the deep North Atlantic. Nature 456: 788–791

Alonso-Sáez L, Waller AS, Mende DR, Bakker K and others (2012) Role for urea in nitrification by polar marine Archaea. Proc Natl Acad Sci USA 109:17989–17994

Amann RI, Ludwig W, Schleifer KH (1995) Phylogenetic identification and in situ detection of individual microbial cells without cultivation. Microbiol Rev 59:143–169

Beal EJ, House CH, Orphan VJ (2009) Manganese- and iron-dependent marine methane oxidation. Science 325: 184–187

Berg C, Beckmann S, Jost G, Labrenz M, Jürgens K (2013) Acetate-utilizing bacteria at an oxic-anoxic interface in the Baltic Sea. FEMS Microbiol Ecol 85:251–261

Bowman JP, McCuaig RD (2003) Biodiversity, community structural shifts and biogeography of prokaryotes within Antarctic continental shelf sediment. Appl Environ Microbiol 69:2463–2483

Bristow LA, Dalsgaard T, Tiano L, Mills DB and others (2016) Ammonium and nitrite oxidation at nanomolar oxygen concentrations in oxygen minimum zone water. Proc Natl Acad Sci USA 113:10601–10606

Canfield DE, Jørgensen BB, Fossing H, Glud R and others (1993) Pathways of organic carbon oxidation in three continental margin sediments. Mar Geol 113:27–40

Canfield DE, Thamdrup B, Kristensen E (2005) Aquatic geomicrobiology. Elsevier, Amsterdam

Danovaro R, Marrale D, Dell'Anno A, Croce ND, Tselepides A, Fabiano M (2000) Bacterial response to seasonal changes in labile organic matter composition on the con-

tinental shelf and bathyal sediments of the Cretan Sea. Prog Oceanogr 46:345–366
Ding J, Wang X, Zhang T, Qingman L, Mingbiao L (2006) Optimization of RP-HPLC analysis of low molecular weight organic acids in soil. J Liq Chromatogr Relat Technol 29:99–112
Durbin AM, Teske A (2010) Sediment-associated microdiversity within the Marine Group I Crenarchaeota. Environ Microbiol Rep 2:693–703
Ehrlich H (1990) Geomicrobiology. Marcel Dekker, New York, NY
Finke N, Vandieken V, Jørensen BB (2007) Acetate, lactate, propionate, and isobutyrate as electron donors for iron and sulfate reduction in Arctic marine sediments, Svalbard. FEMS Microbiol Ecol 59:10–22
Fossing H, Jørgensen BB (1989) Measurement of bacterial sulfate reduction in sediments: evaluation of a single-step chromium reduction method. Biogeochemistry 8: 205–222
Francis CA, Roberts KJ, Berman JM, Santoro AE, Oakley BB (2005) Ubiquity and diversity of ammonia-oxidizing archaea in water columns and sediments of the ocean. Proc Natl Acad Sci USA 102:14683–14688
Fredrickson JK, Romine MF, Beliaev AS, Auchtung JM and others (2008) Towards environmental systems biology of *Shewanella.* Nat Rev Microbiol 6:592–603
Fredriksson NJ, Hermansson M, Wilén BM (2014) Tools for T-RFLP data analysis using Excel. BMC Bioinformatics 15:361
Gillan DC, Danis B (2007) The archaebacterial communities in Antarctic bathypelagic sediments. Deep Sea Res II 54: 1682–1690
Granger J, Prokopenko M, Sigman D, Mordy CW and others (2011) Coupled nitrification-denitrification in sediment of the eastern Bering Sea shelf leads to ^{15}N enrichment of fixed N in shelf waters. J Geophys Res Oceans 116: c11006
Hall PO, Aller RC (1992) Rapid small-volume, flow injection analysis for CO_2 and NH_4^+ in marine and freshwaters. Limnol Oceanogr 37:1113–1119
Henriksen K, Blackburn T, Lomstein B, McRoy CP (1993) Rates of nitrification, distribution of nitrifying bacteria and inorganic N fluxes in northern Bering–Chukchi shelf sediments. Cont Shelf Res 13:629–651
Hyun JH, Kim D, Shin CW, Noh JH and others (2009a) Enhanced phytoplankton and bacterioplankton production coupled to coastal upwelling and an anticyclonic eddy in the Ulleung basin, East Sea. Aquat Microb Ecol 54:45–54
Hyun JH, Mok JS, Cho HY, Kim SH, Lee KS, Kostka JE (2009b) Rapid organic matter mineralization coupled to iron cycling in intertidal mud flats of the Han River estuary, Yellow Sea. Biogeochemistry 92:231–245
Hyun JH, Mok JS, You OR, Kim D, Choi DL (2010) Variations and controls of sulfate reduction in the continental slope and rise of the Ulleung Basin off the southeast Korean upwelling system in the East Sea. Geomicrobiol J 27:212–222
Hyun JH, Kim SH, Mok JS, Cho H, Lee T, Vandieken V, Thamdrup B (2017) Manganese and iron reduction dominate organic carbon oxidation in surface sediments of the deep Ulleung Basin, East Sea. Biogeosciences 14: 941–958
Inagaki F, Suzuki M, Takai K, Oida H and others (2003) Microbial communities associated with geological horizons in coastal subseafloor sediments from the Sea of Okhotsk. Appl Environ Microbiol 69:7224–7235
Inagaki F, Nunoura T, Nakagawa S, Teske A and others (2006) Biogeographical distribution and diversity of microbes in methane hydrate-bearing deep marine sediments on the Pacific Ocean margin. Proc Natl Acad Sci USA 103:2815–2820
Jensen MM, Thamdrup B, Rysgaard S, Holmer M, Fossing H (2003) Rates and regulation of microbial iron reduction in sediments of the Baltic-North Sea transition. Biogeochemistry 65:295–317
Jin T, Zhang T, Ye L, Lee OO, Wong YH, Qian PY (2011) Diversity and quantity of ammonia-oxidizing *Archaea* and *Bacteria* in sediment of the Peral River Estuary, China. Appl Microbiol Biotechnol 90: 1137–1145
Jørgensen BB (1978) A comparison of methods for the quantification of bacterial sulfate reduction in coastal marine sediments, 1. Measurement with radiotracer techniques. Geomicrobiol J 1:11–27
Jørgensen BB (2006) Bacteria and marine biogeochemistry. In: Schulz HD, Zabel M (eds) Marine geochemistry. Springer-Verlag, Berlin Heidelberg, p 169–206
Jørgensen BB, Kasten S (2006) Sulfur cycling and methane oxidation. In: Schultz HD, Zabel M (eds) Marine geochemistry. Springer-Verlag, Berlin Heidelberg, p 271–310
Jorgensen SL, Hannisdal B, Lansén A, Baumberger T and others (2012) Correlating microbial community profiles with geochemical data in highly stratified sediments from the Arctic mid-ocean ridge. Proc Natl Acad Sci USA 109:E2846–E2855
Kim JG (2015) Physiological and evolutionary adaptions of ammonia-oxidizing archaea to oligotrophic environments and oxidative stress. PhD dissertation, Chungbuk National University, Cheongju
Kim D, Choi MS, Oh HY, Kim KH, Noh JH (2009) Estimate of particulate organic carbon export flux using $^{234}Th/^{238}U$ disequilibrium in the southwestern East Sea during summer. The Sea: J Kor Soc Oceanogr 14:1–9 (in Korean with English Abstract)
Könneke M, Bernhard AE, Torre DL, Walker CB, Waterbury JB, Stahl DA (2005) Isolation of an autotrophic ammonia-oxidizing marine archaeon. Nature 437: 543–546
Kostka JE, Roychoudhury A, Van Cappellen P (2002) Rates and controls of anaerobic microbial respiration across spatial and temporal gradients in saltmarsh sediment. Biogeochemistry 60:49–76
Lancaster KM, Caranto JD, Majer SH, Smith MA (2018) Alternative bioenergy: Updates to and challenges in nitrification metalloenzymology. Joule 2:421–441
Lee T, Hyun JH, Mok JS, Kim D (2008) Organic carbon accumulation and sulfate reduction rates in slope and basin sediments of the Ulleung basin, East/Japan Sea. GeoMar Lett 28:153–159
Leloup J, Fossing H, Kohls K, Holmkvist L, Borowski C, Jørgensen BB (2009) Sulfate-reducing bacteria in marine sediment (Aarhus Bay, Denmark): abundance and diversity related to geochemical zonation. Environ Microbiol 11:1278–1291
Lentini CJ, Wankel SD, Hansel CM (2012) Enriched iron(III)-reducing bacterial communities are shaped by carbon substrate and iron oxide mineralogy. Front Microbiol 3:404

Li L, Kato C, Horikoshi K (1999) Bacterial diversity in deep-sea sediments from different depths. Biodivers Conserv 8:659–677

Lovley DR, Phillips EJP (1988) Novel mode of microbial energy metabolism: organic carbon oxidation coupled to dissimilatory reduction of iron or manganese. Appl Environ Microbiol 54:1472–1480

Meng J, Xu J, Qin D, He Y, Xiao X, Wang F (2014) Genetic and functional properties of uncultivated MCG archaea assessed by metagenome and gene expression analyses. ISME J 8:650–659

Moeseneder MM, Winter C, Arrieta JM, Herndl GJ (2001) Terminal-restriction fragment length polymorphism (T-RFLP) screening of a marine archaeal clone library to determine the different phylotypes. J Microbiol Methods 44:159–172

Na T, Thamdrup B, Kim B, Kim SH, Vandieken V, Kang DJ, Hyun JH (2018) N_2 production through denitrification and anammox across the continental margin (shelf-slope-rise) of the Ulleung Basin, East Sea. Limnol Oceanogr 63:S410–S424

Orcutt BN, Sylvan JB, Knab NJ, Edwards KJ (2011) Microbial ecology of the dark ocean above, at, and below the seafloor. Microbiol Mol Biol Rev 75:361–422

Ouverney CC, Fuhrman JA (2000) Marine planktonic archaea take up amino acids. Appl Environ Microbiol 66: 4829–4833

Park SJ, Park BJ, Rhee SK (2008) Comparative analysis of archaeal 16S rRNA and *amoA* genes to estimate the abundance and diversity of ammonia-oxidizing archaea in marine sediments. Extremophiles 12:605–615

Parkes RJ, Gibson GR, Mueller-Harvey I, Buckingham WJ, Herbert RA (1989) Determination of the substrate for sulphate-reducing bacteria within marine and estuarine sediments with different rates of sulphate reduction. J Geo Microbiol 135:175–187

Phillips EJP, Lovley DR (1987) Determination of Fe(III) and Fe(II) in oxalate extracts of sediment. Soil Sci Soc Am J 51:938–941

Probandt D, Knittel K, Tegetmeyer HE, Ahmerkamp S, Holtappels M, Amann R (2017) Permeability shapes bacterial communities in sublittoral surface sediments. Environ Microbiol 19:1584–1599

Qin W, Amin SA, Martens-Habbena W, Walker CB and others (2014) Marine ammonia-oxidizing archaeal isolates display obligate mixotrophy and wide ecotypic variation. Proc Natl Acad Sci USA 111:12504–12509

Radajewski S, Ineson P, Parekh N, Murrell JC (2000) Stable-isotope probing as a tool in microbial ecology. Nature 403:646–649

Redmond MC, Valentine DL, Sessions AL (2010) Identification of novel methane-, ethane- and propane-oxidizing bacteria at marine hydrocarbon seeps by stable isotope probing. Appl Environ Microbiol 76:6412–6422

Roalkvam I, Drønen K, Stokke R, Daae FL, Dahle H, Steen IH (2015) Physiological and genomic characterization of *Arcobacter anaerophilus* IR-1 reveals new metabolic features in *Epsilonproteobacteria*. Front Microbiol 6:987

Rotthauwe JH, Witzel KP, Liesack W (1997) The ammonia monooxygenase structural gene *amoA* as a functional marker: molecular fine-scale analysis of natural ammonia-oxidizing populations. Appl Environ Microbiol 63: 4704–4712

Ruff SE, Arnds J, Knittel K, Amann R, Wegener G, Ramette A, Boetius A (2013) Microbial communities of deep-sea methane seeps at Hikurangi continental margin (New Zealand). PLOS ONE 8:e72627

Sasi Jyothsna TS, Rahul K, Ramaprasad EV, Sasikala C, Ramana C (2013) *Arcobacter anaerophilus* sp. nov. isolated from an estuarine sediment and emended description of the genus *Arcobacter*. Int J Syst Evol Microbiol 63: 4619–4625

Schauer R, Bienhold C, Ramette A, Harder J (2010) Bacterial diversity and biogeography in deep-sea surface sediments of the South Atlantic Ocean. ISME J 4:159–170

Schauer R, Roy H, Augustin N, Gennerich HH and others (2011) Bacterial sulfur cycling shapes microbial communities in surface sediments of an ultramafic hydrothermal vent field. Environ Microbiol 13:2633–2648

Schloss PD, Westcott SL, Thomas R, Hall JR and others (2009) Introducing mothur: open-source, platform-independent, community-supported software for describing and comparing microbial communities. Appl Environ Microbiol 75:7537–7541

Seyler LM, McGuinness LM, Kerkhof LJ (2014) Crenarchaeal heterotrophy in salt marsh sediments. ISME J 8: 1534–1543

Sørensen J (1982) Reduction of ferric iron in anaerobic, marine sediment and interaction with reduction of nitrate and sulfate. Appl Environ Microbiol 43:319–324

Spang A, Saw JH, Jørgensen SL, Zaremba-Niedzwiedzka K and others (2015) Complex archaea that bridge the gap between prokaryotes and eukaryotes. Nature 521: 173–179

Stookey LL (1970) Ferrizine — a new spectrophotometric reagent for iron. Anal Chem 42:779–781

Teira E, van Aken H, Veth C, Herndl GJ (2006) Archaeal uptake of enantiomeric amino acids in the meso- and bathypelagic waters of the North Atlantic. Limnol Oceanogr 51:60–69

Thamdrup B, Canfield DE (1996) Pathways of carbon oxidation in continental margin sediments off central Chile. Limnol Oceanogr 41:1629–1650

Thamdrup B, Canfield DE (2000) Benthic respiration in aquatic sediment. In: Sala OE, Jakson RB, Mooney HA, Howarth RW (eds) Methods in ecosystem science. Springer-Verlag, Berlin Heidelberg, p 86–103

Thamdrup B, Rosselló-Mora R, Amann R (2000) Microbial manganese and sulfate reduction in Black Sea shelf sediments. Appl Environ Microbiol 66:2888–2897

Vandieken V, Thamdrup B (2013) Identification of acetate-oxidizing bacteria in a coastal marine surface sediment by RNA-stable isotope probing in anoxic slurries and intact cores. FEMS Microbiol Ecol 84:373–386

Vandieken V, Nickel M, Jørgensen BB (2006) Carbon mineralization in Arctic sediments northeast of Svalbard: Mn(IV) and Fe(III) reduction as principal anaerobic respiratory pathways. Mar Ecol Prog Ser 322:15–27

Vandieken V, Pester M, Finke N, Hyun JH, Friedrich MW, Loy A, Thamdrup B (2012) Three manganese oxide-rich marine sediments harbor similar communities of acetate-oxidizing manganese-reducing bacteria. ISME J 6: 2078–2090

Vetriani C, Jannasch HW, MacGregor BJ, Stahl DA, Reysenbach AL (1999) Population structure and phylogenetic characterization of marine benthic archaea in deep-sea sediments. Appl Environ Microbiol 65:4375–4384

Webster G, Rinna J, Roussel EG, Fry JC, Weightman AJ, Parkes RJ (2010) Prokaryotic functional diversity in different biogeochemical depth zones in tidal sediments of

the Severn Estuary, UK, revealed by stable-isotope probing. FEMS Microbiol Ecol 72:179–197

Whiteley AS, Thomson B, Lueders T, Manefield M (2007) RNA stable-isotope probing. Nat Protoc 2:838–844

Wuchter C, Abbas B, Coolen MJL, Herfort L and others (2006) Archaeal nitrification in the ocean. Proc Natl Acad Sci USA 103:12317–12322

Yao W, Millero FJ (1996) Oxidation of hydrogen sulfide by hydrous Fe(III) oxides in seawater. Mar Chem 52:1–16

Yoo S, Park J (2009) Why is the southwest the most productive region of the East Sea/Sea of Japan? J Mar Syst 78: 301–315

Zeleke J, Sheng Q, Wang JG, Huang MY, Xia F, Wu JH, Quan ZX (2013) Effects of *Spartina alterniflora* invasion on the communities of methanogens and sulfate-reducing bacteria in estuarine marsh sediments. Front Microbiol 4:243

Editorial responsibility: Toshi Nagata, Kashiwanoha, Japan

Submitted: November 30, 2018; Accepted: November 4, 2019
Proofs received from author(s): January 15, 2020